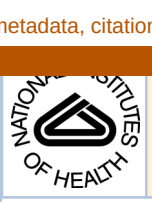

Published in final edited form as:

Chem Biol. 2010 July 30; 17(7): 695–704. doi:10.1016/j.chembiol.2010.04.014.

Accessing Protein Methyltransferase and Demethylase Enzymology Using Microfluidic Capillary Electrophoresis

Tim J. Wigle[1], **Laurel M. Provencher**[2], **Jacqueline L. Norris**[1], **Jian Jin**[1], **Peter J. Brown**[3], **Stephen V. Frye**[1], and **William P. Janzen**[1]

[1] Center for Integrative Chemical Biology and Drug Discovery, Division of Medicinal Chemistry and Natural Products, Eshelman School of Pharmacy, The University of North Carolina, 2092 Genetic Medicine Building CB #7363, 120 Mason Farm Rd, Chapel, Hill, North Carolina, 27599-7363

[2] Caliper Life Sciences, 68 Elm Street, Hopkinton, Massachusetts, 01748

[3] Structural Genomics Consortium, University of Toronto, MaRS Centre South Tower, 101 College St., Suite 700, Toronto, Ontario, M5G 1L7

Summary

The discovery of small molecules targeting the > 80 enzymes that add (methyltransferases) or remove (demethylases) methyl marks from lysine and arginine residues, most notably present in histone tails, may yield unprecedented chemotherapeutic agents and facilitate regenerative medicine. To better enable chemical exploration of these proteins, we have developed a novel and highly quantitative microfluidic capillary electrophoresis assay to enable full mechanistic studies of these enzymes and the kinetics of their inhibition. This technology separates small biomolecules, *i.e.*, peptides, based on their charge-to-mass ratio. Methylation, however, does not alter the charge of peptide substrates. To overcome this limitation, we have employed a methylation-sensitive endoproteinase strategy to separate methylated from unmethylated peptides. The assay was validated on a lysine methyltransferase (G9a) and a lysine demethylase (LSD1) and was employed to investigate the inhibition of G9a by small molecules.

Introduction

The epigenetic code is written on DNA in the form of methylation, and on histone proteins as methylation, acetylation, phosphorylation, ubiquitination, sumoylation and ADP-ribosylation (Gelato and Fischle, 2008). The four main histone proteins (H2A, H2B, H3 and H4) form an octomeric unit around which 147 bp of DNA are wrapped to make a nucleosome, which is the repeating unit of chromatin. Histone proteins contain flexible N-terminal tails that protrude from the nucleosome core where the bulk of these post-translation modifications are “written”, “read” and “erased” by a myriad proteins. The most commonly modified residues are lysine, which can be acetylated or methylated, and arginine, which can be methylated. The pattern of modifications influences chromatin architecture, ultimately controlling the temporal and spatial access of transcription factors to specific genes (Kouzarides, 2007).

Address correspondence to William P. Janzen; bjanzen@email.unc.edu, tel: 919-843-8461, fax: 919-843-8465.

Since the discovery of the first histone lysine methyltransferase in 2000 (Rea et al., 2000), > 50 protein lysine methyltransferases (PKMTs) and > 10 protein arginine methyltransferases (PRMTs) have been identified. These enzymes transfer a methyl group from the cofactor *S*-adenosylmethionine (SAM) to the ε-amino group of lysine or the guanidine group of arginine, most likely through an S_N2 mechanism where the lone pair of electrons on nitrogen attack the electrophillic methylsulfonium group on SAM, producing the byproduct *S*-adenosylhomocysteine (SAH) (Copeland et al., 2009). Lysine residues can be mono-, di-, or trimethylated, while the guanidine group of arginine can be monomethylated, asymmetrically dimethylated, or symmetrically dimethylated. In addition, since the first histone demethylase was discovered in 2004 (Shi et al., 2004), at least 30 enzymes belonging to this family have been identified (Copeland et al., 2009) and indicate that histone methylation is a dynamic process. Among the demethylating enzymes, there are the flavin-dependent monoamine oxidases like LSD1, and the JmjC domain demethylases. LSD1-like demethylases convert mono- or di- but not trimethylated amino groups to imines that are subsequently non-enzymatically hydrolyzed, while JmjC-domain demethylases utilize iron and α-ketoglutarate cofactors to hydroxylate mono-, di or trimethyl lysines (Trewick et al., 2005) and even methylated arginines (Chang et al., 2007). In both cases, the hydroxylated methyl groups spontaneously hydrolyze, releasing formaldehyde, the by-product of catalysis that retains the carbon of the oxidized methyl group. While the activity of protein methyltransferases and demethylases is synonymous with histone modification, there is increasing evidence for their role in modification of other nuclear and cytosolic proteins such as p53 (Huang et al., 2007; Huang et al., 2010), various transcription factors (Couture et al., 2006), WIZ, histone deacetylases, DNA methyltransferases and even the protein methyltransferases themselves (Rathert et al., 2008). Recognition of methyl-lysine marks has been associated with the “Royal Family” of proteins including those containing Tudor, Chromo, Maligant Brain Tumor (MBT), PWWP, and plant Agenet domains, the plant homeodomain (PHD) family and the WD40 repeat protein WRD5. These motifs all have structurally related binding pockets defined by an aromatic electron-rich cage and H-bond donors that interact with the lysine cation (Adams-Cioaba and Min, 2009). Many chromatin-acting enzymes, including a vast number that modify histones, contain these domains that recruit them to their site of action, and the development of small molecule antagonists of methyl-lysine recognition is another area of active interest (Wigle et al., 2010).

The bioorthogonal relationship between protein methyltransferases and protein demethylases influences how the histone code is read by methyl-lysine binding proteins and ultimately has a profound effect on the pattern of gene expression in a particular cell. Mounting evidence suggests that many diseases are rooted in epigenetic misregulation, and that therapies targeting epigenetic processes may be a revolutionary strategy to combat illness in the future (Cole, 2008; Keppler and Archer, 2008). It is known that overexpression of any one of a number of protein methyltransferases or demethylases can lead to a variety of cancers (Copeland et al., 2009; Spannhoff et al., 2009a), inflammation (Li et al., 2008), cardiovascular disease (Chen et al., 2006) and neurological disorders (Tahiliani et al., 2007). In addition, these enzymes are fundamental to cellular fate, and may be manipulated in cellular reprogramming efforts (Shi et al., 2008a; Shi et al., 2008b). Therefore, high quality chemical probes (Frye, 2010) of protein methyltransferases and demethylases will enhance our understanding of their potential as therapeutic targets, and may ultimately lead to pharmacological agents for a variety of afflictions.

To facilitate the development of chemical probes for the enzymes that write and erase histone methyl marks, we have developed a highly quantitative microfluidic capillary electrophoresis (MCE) assay that distinguishes between methylated and unmethylated histone peptides, and provides mechanistic insight into the inhibition of these enzymes by

small molecules. MCE operates on the principle that small biomolecules taken from nanoliter-sized aliquots of reaction samples are separable in a capillary quartz channel based on their charge-to-mass ratio when a current is applied. This technique can be performed in high-throughput fashion and has been adopted as a gold standard assay in the profiling of small molecule inhibitors of kinases, proteases, and histone acetyltransferases (HATs) and deacetylases (HDACs), which modify the isoelectric points of their peptide substrates.

Methylation, however does not alter the charge-to-mass ratio of peptide substrates. To overcome this hurdle to assay development on this highly quantitative platform, we have employed a methylation-sensitive protease cleavage strategy to distinguish between methylated and unmethylated peptides. The ratio of substrate-to-product peak sizes is determined, providing very accurate and reproducible measurements of conversion, and detailed insights into enzyme kinetics. Parameters such as K_i, K_m and k_{cat} can be measured with confidence and the mechanism of action of putative inhibitors can be probed, enhancing the efficacy of compound profiling efforts in the early stages of drug discovery. These advantages distinguish this assay format over other methods, such as the incorporation of radioactive methyl groups using ^{3}H-SAM, AlphaScreen (Quinn et al., 2010) and ELISA-based detection (Kubicek et al., 2007) of methylated peptide substrates, and enzyme-coupled measurement of SAH production (Collazo et al., 2005). These techniques either suffer from an inability to generate high quality kinetic data, or are difficult to automate, and in the case of radioactive assays, can be hazardous to the operator. We applied this assay to G9a, a lysine methyltransferase, and LSD1, a lysine demethylase, demonstrating a broad potential for the application of this assay to enzymes that alter the methylation state of peptide substrates. Therefore, microfluidic capillary electrophoresis represents a sophisticated methodology capable of establishing a new standard in both the precision and accuracy with which small molecule inhibitors of protein methyltransferases and demethylases are identified and evaluated.

Experimental Procedures

Materials

Endoproteinase-LysC (Endo-LysC) was obtained as a lyophilized powder from Pierce via Thermo Fisher Scientific (Waltham, MA) and resuspended to a concentration of 1 ng/μL in 25 mM Tris-HCl (pH = 8) then aliquoted and stored at −80 °C. 384-well V-bottom polypropylene microplates were purchased from Greiner (Monroe, NC) and 384-well low volume shallow microplates were purchased from Nunc via Thermo Fisher Scientific (Waltham, MA). *S*-adenosylmethionine (SAM) was purchased from New England Biolabs (Ipswich, MA). Sinefungin was purchased from Sigma-Aldrich (St. Louis, MO) and all other reagents were obtained from Fisher Scientific. Inhibitors of G9a methyltransferase used in assay development were synthesized in our laboratory and will be published with full chemical characterization elsewhere. The catalytic domain of G9a (residues 913–1193) was purified as previously described (Wu et al., 2010). LSD1 was purchased from two different sources: BPS Biosciences (San Diego, CA) and Enzo Life Sciences (Farmingdale, NY). In all cases the assay buffer used was 20 mM Tris-HCl, 25 mM NaCl, 0.025 % Tween 20 and 1 mM DTT [pH = 8].

Peptides

Several peptides containing a 5/6-carboxyfluorescein tracer (5/6-FAM, abbreviated to FAM below) were used in assay development. All peptides were synthesized and high-performance liquid chromatography (HPLC)-purified by either the Tufts University Peptide Synthesis Core Facility (Boston, MA) or Intonation Technologies (West Roxbury, MA) and contained N-terminal amino and C-terminal amide groups. The inclusion of a

monomethylated lysine is indicated by K(me1). Two peptides, QTARKSTGGK(FAM) **(1)** and QTARK(me1)STGGK(FAM) **(5)** were used in the proof-of-principle experiments to validate the methylation-sensitive endoproteinase-coupled assay strategy. The optimized G9a substrate was the histone H3 peptide ARTK(me1)QTARKSTGGK(FAM) **(2)**. Two peptides representative of histone H3 were tested for LSD1 activity, ARTK(me1)QTARASTGGAAPRAQLAK(FAM) and **(3)** ARTK(me1)QTARK(FAM)STGGKAPRKQLAK **(4)**.

G9a Lysine Methyltransferase Assays

Methylated and unmethylated peptides were separated following endoproteinase digestion on a Caliper LabChip EZ Reader II equipped with a 12-sipper chip in ProfilerPro separation buffer supplemented with CR-8 and analyzed using EZ Reader software (Caliper Life Sciences; Hopkinton, MA). The initial G9a activity assay was performed in a microcentrifuge tube by pre-mixing G9a and peptide **2**, and initiating the reaction with the addition of 50 μM SAM. Timepoints (10 μL) were sampled with and without a heatkill step (5 min exposure to 80 °C) and added to 40 pg/μL Endo-LysC in a 384-well V-bottom polypropylene microplate. The measurement of G9a methyltransferase kinetics was performed in 50 or 15 μL volumes in 384-well polypropylene V-bottom or shallow microplates using 25 nM G9a and either 50 μM SAM or 50 μM peptide **2**, and initiated by addition of either SAM or peptide **2**. Parallel reactions were set up and allowed to proceed at 25 °C, and aliquots were analyzed by stopping the reaction with 10 μL of a cocktail Endo-LysC (40 pg/μL) and UNC0224 (Liu et al., 2009) (5 μM), which was added to immediately inhibit all further enzyme activity. Inhibitor-substrate competitions were set up similarly, and the contribution of DMSO concentration from compound addition was maintained at 1 %. All dose-response assays (IC_{50}'s) of putative G9a inhibitors were set up by pre-incubating a cocktail of 25 nM G9a and 5 μM peptide with the inhibitors for 10 min at 25 °C, and initiated by the addition of 10 μM SAM. The concentration of DMSO was maintained at 1 %, and minimum signal controls were run in the absence of SAM. After incubation for 1 h at 25 °C, 40 pg/μL Endo-LysC was added and allowed to digest the remaining unmethylated substrate peptide (and the G9a) for at least 30 min prior to separation on the EZ Reader II. The separation of peptide **2** was performed under the following optimized conditions: upstream voltage = −500 V, downstream voltage = −1200 V and pressure = −1.5 psi using a marker dye consisting of peptide **2** that was completely pre-digested with Endo-LysC.

LSD1 Lysine Demethylase Assays

The measurement of LSD1 kinetics was performed in a microcentrifuge tubes, and initiated by adding peptide **4** to LSD1 and allowed to proceed at 25 °C. Aliquots (10 μL) were sampled at various timepoints both with and without a heatkill step (5 min exposure to 80 °C) and added to 40 pg/μL Endo-LysC in a 384-well shallow microplate with proteolysis of the methylated substrate peptide (and the LSD1) for at least 30 min prior to separation on the EZ Reader II. The separation of peptide **4** was performed under the following optimized conditions: upstream voltage = −500 V, downstream voltage = −2000 V and pressure = −1.7 psi using a marker dye consisting of peptide **4** that was pre-digested with Endo-LysC.

Data Analysis

Enzyme kinetics and parameters such as K_m and K_i were determined using Prism software (GraphPad Software Inc, San Diego, CA) to analyze Michaelis-Menten fits of initial enzyme velocities. Automated dose-response runs were analyzed using ScreenAble software (Screening Solutions LLC, Chapel Hill, NC) and IC_{50} values and Hill Slopes were generated using 4-parameter fits. The quality and robustness of the assay was determined by analysis of the Z′ factor (Zhang et al., 1999):

$$Z' = 1 - \left(\frac{3\sigma_{max} + 3\sigma_{min}}{|\mu_{max} - \mu_{min}|} \right)$$

where σ_{max} and σ_{min} are standard deviations of the respective maximum and minimum signal controls, and μ_{max} and μ_{min} are the averages of the respective maximum and minimum signal controls.

Results

Detection of Methylation-Sensitive Peptide Cleavage

Since methylation does not alter the electrophoretic properties of peptides, an endoproteinase-coupled strategy was used to distinguish between unmethylated and methylated histone peptides in a microfluidic mobility shift assay. Endoproteinase-LysC (Endo-LysC) cleaves peptide bonds that are on the C-terminal side of lysine residues, and is commonly used in mass spectrometric analysis of proteins. Recently, Boa et al. reported that the mass spectrometry profiles of Endo-LysC digested histone H3 extracted from yeast cells having a *set1* methyltransferase knockout differed greatly from extracts of wild-type cells, and hypothesized that the Endo-LysC was unable to cleave after methylated lysines (Boa et al., 2003). Therefore, we surmised that methylation-sensitive endoproteinase cleavage could be a novel method to assay histone methylation and demethylation in the context of an *in vitro* assay.

To verify that Endo-LysC would selectively cleave peptides after unmodified lysines, an initial experiment was designed using two synthetic peptides labeled with fluorescein that are representative of unmethylated and monomethylated lysine 9 on histone H3 (H3K9me1). Different ratios of the unmethylated (**1**) and monomethylated (**5**) peptides were mixed such that the total peptide concentration was 1 μM, Endo-LysC was added, and electrophoretic separation of the reaction products was performed. It was observed that Endo-LysC was unable to cleave the peptide containing the monomethylated lysine, but was able to fully cleave > 97 % of the peptide containing the unmodified lysine in less than 1 hr, indicated by the appearance of a second peak (Figure 2A). The amount of methylated peptide detected corresponded well with the calculated amount of methylated peptide actually added (Figure 2B).

Design of Substrates for Methyltransferase and Demethylase Enzymes

Having established that MCE could be used to distinguish between methylated and unmethylated peptides, the next step was to demonstrate that this assay could be used to monitor the activity of enzymes that alter the methylation state of peptide substrates (Figure 3). In designing substrates, it is important to consider the position of the fluorescein tracer relative to the location of Endo-LysC susceptible lysine residues to balance substrate turnover with the ease of electrophoretic separation (Figure 3D). The first and most straightforward example of this strategy is the design of a substrate for G9a (EHMT2). G9a targets lysine 9 on histone peptide H3, and has been shown to be sensitive to certain changes in the residues flanking the target site (Rathert et al., 2008). Initial attempts to use peptide **1** (the 8mer peptide spanning residues 5–14 of the H3 peptide) as a G9a substrate, did not result in methylation-dependent protection from Endo-LysC digestion (data not shown). To investigate whether the peptide length and omission of residues 1-4 of the histone H3 peptide was responsible for the lack of G9a activity, a longer peptide (**2**) spanning residues 1-14 of the H3 peptide was synthesized, with fluorescein on the terminal K14 residue. To simplify the analysis of cleavage products, lysine 4 was pre-methylated during synthesis of

the peptide to prevent Endo-LysC digestion at this position. Using peptide **2** as substrate for lysine 9 methylation, robust protection of peptide cleavage was observed, corresponding to G9a methyltransferase activity (Figures 3A & 3B). The velocity of three reactions with different G9a concentrations was measured by taking aliquots at various timepoints with or without a heatkill step to deactivate the enzyme. The reaction velocities obtained by either method corresponded well, with slightly higher conversion observed for reactions without a heatkill step. We concluded that heatkill is not necessary when looking at relative G9a kinetics, for example the determination of inhibitor IC_{50} values, as the presence of 40 pg/μL Endo-LysC rapidly digests both the peptide and G9a, concluding the reaction. However, as described in the following sections, when examining absolute kinetic parameters for G9a, such as K_m, k_{cat} and K_i, we found that terminating the reaction with a cocktail of Endo-LysC and a known G9a inhibitor, UNC0224, produced the best results.

To further demonstrate the applicability of this assay concept across the families of enzymes that alter the methylation state of histone peptides, we explored the possibility of monitoring the activity of LSD1 (AOF2), a lysine demethylase. For LSD1, substrate design was more complex than in the case of G9a, and several factors were taken into consideration. LSD1 is known to demethylate mono- and dimethyl lysine 4 of histone H3 peptide (H3K4me1/2) and previous reports have shown that LSD1 activity is commensurate with longer peptides that span at least 20 residues (Forneris et al., 2005). However, the H3 peptide spanning residues 1-22 contains multiple lysines that could be subject to cleavage by Endo-LysC and it is advantageous to avoid placing the fluorescein label close to the site of demethylation in order to retain maximum substrate turnover. To address these considerations in LSD1 substrate design, two H3 peptides spanning residues 1-22 were evaluated. Both peptides were synthesized with monomethylation at lysine 4, and one peptide had all other lysines replaced by alanine except for lysine 22, which contained the fluorescein group (peptide **3**), while the other peptide kept all lysines intact, and fluorescein was included internally on lysine 9 (peptide **4**). In the case of peptide **4**, it was expected that all other lysines would undergo cleavage, but the fluorescein label on lysine 9 would prevent proteolysis at that position. Therefore, the success of the assay using peptide **4** would rely on the separation of peptides spanning residues 1-14 or 5-14 depending on the activity of LSD1. Ultimately, peptide **3** having all other lysines substituted for alanines was not demethylated by LSD1, but peptide **4** having an internally fluoresceinated lysine 9, led to the detection of robust and linear LSD1 activity. Again, three concentrations of LSD1 were reacted with 2 μM peptide **4** and timepoints were sampled with or without a heatkill step (Figure 3C). We observed that for small molecule screening, a heatkill step is not necessary.

Measurement of G9a Lysine Methyltransferase Kinetics

After demonstrating that we could detect time-dependent G9a methylation of peptide **2**, the use of the assay was extended to the measurement of kinetic parameters K_m and k_{cat}. Reactions containing titrations of either SAM or the peptide were monitored as a function of time. The conversion of substrate to product was determined, and subjected to a linear regression analysis (Figures 4A & 4B) to measure the initial velocities of the reaction as a function of the titrant concentration (Figures 4C & 4D). Between both experiments, the following parameters were calculated: k_{cat} of 13 ± 3 min^{-1}, K_m^{SAM} of 31.7 μM and $K_m^{peptide}$ of 36.2 μM. The affinity for both substrates was similar, as were the maximal reaction velocities, consistent with this reaction proceeding as a bimolecular S_N2 mechanism (Copeland et al., 2009).

Configuring the G9a Methyltransferase Assay for Small Molecule Screening

Microfluidic capillary electrophoresis assays on the Caliper LabChip platform are used in the pharmaceutical industry for small molecule screening and profiling of protein target

classes such as kinases, phosphodiesterases, HDACs, HATs and proteases. The reliable and robust performance of this assay platform is well-suited for the screening of chemical libraries and profiling of hits in the early stages of drug discovery so that potential leads can be confidently assessed for potency and selectivity. To take advantage of this assay platform in our ongoing efforts to develop potent and selective chemical probes of PKMTs (Liu et al., 2009), the assay was miniaturized and automated for use with small molecules. Since DMSO is the universal solvent used in small molecule screening, the DMSO tolerance of the G9a assay was determined (Figure 5A). Both Endo-LysC and G9a retained nearly full activity at up to 10% DMSO, making this assay well-suited for both routine screening of small molecules at the standard concentration of 1% DMSO, and in fragment-based screens where the compounds are added at higher concentrations, which requires the presence of elevated DMSO concentrations.

Using low-volume 384-well microplates, the assay volume was decreased more than three-fold (50 μL to 15 μL), thereby saving valuable protein and reagents. The workflow was greatly accelerated by the use of a multidrop dispenser to add reagents to the 384-well plates. To examine the robustness of this automated assay, the methylation of peptide **2** in minimum and maximum control reactions was recorded on two 384-well plates on consecutive days, where the minimum signal control is performed in the absence of SAM. An average Z′ factor (Zhang et al., 1999) of 0.92 was determined with CV values of less than 2%, indicating that this assay is suitable for small molecule screening (Figure 5B).

Our group has explored the structure-activity relationship of compounds based upon the quinazoline template of BIX-01294, a validated cell-permeable inhibitor of G9a and GLP methyltransferases (Kubicek et al., 2007). A co-crystal structure of BIX-01294 bound to GLP, which is more than 80% homologous to G9a in the catalytic domain (Chang et al., 2009), was used to guide initial efforts. In particular, substitutions at the 7-methoxy position of the quinazoline were made to explore the possibility of extending groups into the lysine binding channel of G9a, and the benzyl group that did not make any favorable interactions with the protein was removed (Figure 5E). This led to the discovery of UNC0224, which is more potent than BIX-01294 and is the first small molecule inhibitor to be co-crystallized with G9a (Liu et al., 2009). The high-resolution X-ray structure of UNC0224 bound to G9a confirmed that its 7-dimethylamino propoxy substituent occupied the lysine binding channel, leading to greatly enhanced affinity for the enzyme. To gauge the ability of this assay to support further probe discovery efforts, the dose-responsive inhibition of G9a by 83 quinazoline-based inhibitors was assessed. While the structure-activity profile generated is beyond the scope of this paper and will be presented in full detail elsewhere, we report excellent correlation between the IC_{50} values obtained in two independent runs of the assay (Figure 5C). However, as shown in Figure 5D, two groups of compounds were evident: (1) those having a Hill Slope of close to 1, with IC_{50} values spanning a range of 5 nM to 30 μM, and (2) compounds with Hill slopes of greater than 1, with IC_{50} values of less than 5 nM. A steep Hill Slope is indicative that the assay potency limit has been exceeded, with the theoretical limit of IC_{50} detection for tight binding inhibitors to be half the total enzyme concentration (Copeland, 2000), which in this case is 10 nM G9a. Strategies for investigating the rank order of these very potent compounds and their mechanism of action are outlined below.

Determination of K_i of UNC0224 vs. Peptide 2

Approximately 25% of the compounds synthesized in the UNC0224 series reached the potency limit of the assay. The co-crystal structure of G9a and UNC0224 (PDB 3K5K), which is at least 10-fold more potent than BIX-01294, guided further inhibitor design. While diversity or fragment-based screening would normally be performed at 500 nM peptide using this assay, quinazoline analogs were screened at 5 μM of competing peptide substrate

to enhance the ability to resolve more potent compounds. Nonetheless, the potency limit of the assay was exceeded by a substantial number of compounds tested, therefore competitive K_i's were determined for this interaction. Using UNC0224 as a benchmark, the compound was titrated using a 1.5-fold dilution scheme from 13.3 nM to 0.7 nM, and aliquots were sampled at various timepoints by adding a cocktail of Endo-LysC and a saturating concentration (5 μM) of UNC0224 to stop the reaction immediately. Fitting the initial rates of reaction observed at each peptide concentration to Michaelis-Menten kinetics yielded parameters associated with the peptide, K_m and V_{max}, which were plotted as a function of the UNC0224 concentration (Figure 6). This confirmed that UNC0224 is competitive with the peptide substrate, as the K_m increased linearly with UNC0224 concentration and the V_{max} remained unchanged. A linear regression of the observed K_m at each UNC0224 concentration was performed, and using the relationship $K_i = K_m/\text{slope}$, the K_i of UNC0224 was determined to be 1.6 nM.

Profiling SAM Competition Using a Rapid Endpoint-Based Variation of the G9a Assay

To expand the diversity of known G9a inhibitors both focused and diversity-based chemical libraries should be screened. In order to differentiate compounds with other possible modes of inhibition including SAM-competitive or allosteric regulators, a rapid endpoint method for profiling SAM-competitive inhibitors was developed. In contrast to the determination of the absolute K_i through time-dependent analysis of methyltransferase reactions, the goal was to use minimal reagent while generating kinetic fingerprints of inhibitors that would allow assessment of the mechanism of inhibition, *i.e.*, competitive with SAM or the peptide, or non-competitive with either. Since the peptide is the most costly reagent in the assay, running full K_i's for SAM competition would be prohibitive as it would require saturating concentrations of roughly 50 μM. To reduce the peptide requirement, K_m^{app} and V_{max}^{app} for SAM were determined at multiple inhibitor concentrations using only 500 nM peptide. The apparent K_m for SAM at 500 nM peptide was 294 ± 3 nM in the absence of inhibitor, about 100-fold less than the absolute K_m, and the V_{max}^{app} measured under these conditions was 7.4 ± 0.1 nM/min, about 60-fold less than the absolute V_{max}. To test this method for comparing inhibition modes, the concentration-dependence of K_m^{app} and V_{max}^{app} was determined for UNC0224, and Sinefungin, a known SAM-competitive inhibitor of methyltransferases (Figure 7). Indeed, Sinefungin displayed a typical SAM-competitive profile where K_m^{app} increased with compound concentration, while V_{max}^{app} remained relatively unchanged, and K_i^{app} for Sinefungin was 18 μM. UNC0224 appeared to be non-competitive with SAM, with K_m^{app} remaining constant with increasing compound concentration, while the V_{max}^{app} decreased asymptotically.

Discussion

Epigenetics is an emerging area of drug discovery that may expand approaches to treat diseases with small molecules. Currently there are only four FDA approved drugs that target the enzymes that regulate the modification state of chromatin, suberoylanilide hydroxamic acid (SAHA, Vorinostat) and Romidepsin (Istodax), which reversibly inhibit histone deacetylases (HDACs), and 5-aza-2′ deoxycytidine\5′-azacytidine (Decitabine\Vidaza), which target DNA methyltransferases irreversibly after incorporation into DNA by polymerase. The discovery of these drugs was fortuitous, arising from phenotypic observations, where the identity of the cellular target was not initially appreciated (Friedman, 1979; Marks, 2007). The eventual link between the cellular targets of these drugs and their therapeutic utility has attracted much attention to the small molecule manipulation of chromatin-regulating proteins and there are now entire research programs and private enterprises devoted to the discovery of small molecules that act upon epigenetic targets (Karberg, 2009). The link between the misregulation of histone methylation and a variety of

diseases (Spannhoff et al., 2009b) and the availability of high resolution X-ray structures for many of these proteins (Marmorstein and Trievel, 2009) are aligned to stimulate and enable the discovery of small molecules that regulate these enzymes. In addition, opportunities to modulate non-histone proteins, *i.e.*, p53 is known to be the target of both G9a (Huang et al., 2010) and LSD1 (Huang et al., 2007), provide both increased therapeutic potential and a challenge to understanding the selectivity and *in vivo* mechanism of action of inhibitors. The precedent that lysine acetylation is now rivaling protein phosphorylation in importance, suggests that we are only beginning to realize the implications of lysine methylation and its consequences for cellular signaling and metabolism (Norvell and McMahon, 2010). High quality chemical probes will undoubtedly play a major role in expanding knowledge in this area (Frye, 2010).

Currently, there are several biochemical assays available that are capable of supporting early stage research for the discovery of potent and selective inhibitors of the enzymes that regulate protein lysine methylation. However, these methods can be hazardous to the operator (radioactivity assays), can be hard to automate (Thioglo assay), or lack the ability to measure enzyme kinetics and are susceptible to compound interference (AlphaScreen). Here, a robust and highly quantitative microfluidic capillary electrophoresis platform is detailed for the study of protein lysine methyltransferase and demethylase enzymology and the effect that small inhibitors have on these enzymes. The assay works by taking advantage of the fact that Endo-LysC, which cleaves peptide bonds on the C-terminal side of lysine residues, is inhibited by lysine methylation. Using a rational approach to the design of peptide substrates, the viability of this assay format was demonstrated for the study of G9a lysine methyltransferase and LSD1 lysine demethylase. The positions of the Endo-LysC susceptible residues and the fluorescein tracer were optimized for substrate turnover, while balancing electrophoretic separation on a Caliper Life Sciences EZ Reader II. The G9a and LSD1 substrates presented here may also serve as model substrates for extending this assay to other enzymes that act on the same residues, H3K9 and H3K4 (experiments underway). In addition, the activity of PRMT3, a protein arginine methyltransferase, was detected using endoproteinase-ArgC to differentiate between unmethylated and methylated arginine (data not shown) and optimization is ongoing. This technique is advantageous for the investigation of methylation and demethylation due to its versatility in both primary high-throughput screens and hit-to-lead optimization. As opposed to radioactive assays, bulk reagents can be safely handled, permitting large scale diversity screening. The fluorescein tracer used to detect both substrate and product is not as susceptible to compound interference as the signal transduction cascade of AlphaScreen or the Thioglo chromophore. In addition, unlike the Thioglo method, the assay performs well as a miniaturized and automated assay, and it far exceeds the ability of AlphaScreen to measure kinetics.

The G9a assay was configured for small molecule inhibitor screening, having a Z′ factor 0.92 and excellent robustness and reproducibility. The assay is well suited to support screening and compound profiling activities as demonstrated using a collection of 83 small molecule analogs of UNC0224 (Liu et al., 2009) to study the inhibition of G9a (Figure 5). While the structure-activity relationship of these compounds is beyond the scope of this paper and will be presented elsewhere, the assay reproducibly rank ordered the compounds in independent runs. However, it was also noticed that compounds clustered into two groups: (1) compounds with Hill slope ≈ 1 and IC_{50} > 5 nM, and (2) ultra-potent peptide-competitive inhibitors, indicated by a Hill slope > 1 and IC_{50} < 5 nM. The original template, BIX-01924 belongs to cluster 1, while UNC0224 falls into cluster 2, and this assay permitted the rigorous characterization of UNC0224. UNC0224 is competitive with the peptide substrate, having a K_i of 1.6 nM, consistent with the binding mode in the co-crystal structure of UNC0224 with G9a (Liu et al., 2009). Additionally, an abbreviated method was used to confirm that UNC0224 was non-competitive with SAM, while Sinefungin was

competitive with SAM, exhibiting a K_i^{app} of 18 μM. Taken together, this appears to be a highly effective method to analyze the effect of small molecules on these enzyme families.

This methylation-sensitive endoproteinase cleavage assay performed on an MCE platform is a practical and highly quantitative method to study the kinetics of protein lysine methyltransferases and demethylases that take peptides from an unmethylated state to methylated state or vice versa. However, it is not applicable to enzymatic reactions that do not involve an unmethylated state in the substrate or product. It is envisioned that research groups without access to a Caliper EZ Reader II will be able to employ a variation of the methylation-sensitive endoproteinase assay strategy on fluorescence polarization (FP), fluorescence resonance energy transfer (FRET) or AlphaScreen platforms.

Significance

Post-translational modifications of histone proteins form the basis of the epigenetic code, which controls the structural state of chromatin and influences gene expression profiles from cell to cell. The enzymes responsible for writing, reading and erasing these modifications are important targets for chemical biology and drug discovery due to their roles in stem cell biology and the etiology of numerous diseases. In particular, the discovery of small molecules targeting the > 80 enzymes that add (methyltransferases) or remove (demethylases) methyl marks from lysine and arginine residues present in histone tails may yield novel therapeutics. To advance our chemical biology efforts in the design of modulators of histone methylation, we have developed a novel assay for protein methyltransferases and demethylases that is well-suited for the profiling of small molecules for potency and selectivity among enzyme family members.

Microfluidic capillary electrophoresis is advantageous for its ability to monitor the formation of product and disappearance of substrate, delivering highly quantitative results and enhancing the sensitivity of assays configured for this platform. However, monitoring lysine methylation presents a challenge for this technique: methylation does not alter the isoelectric properties of peptides substantially and therefore substrates and products of methylation/demethylation reactions are not separable. In this work, methylation-sensitive endoproteinase-cleavage is used as a tool to enable the application of this technology to examine the kinetics of protein methyltransferases and demethylases. This technique was used to profile both peptide- and SAM-competitive inhibitors of G9a methyltransferase in addition to enabling the measurement of K_i values and rank-ordering of inhibitor potency. This assay is well suited to drive both high-throughput screening and chemical biology efforts towards the development of potent and selective modulators of protein methylation.

Highlights

- Novel assay developed for lysine methyltransferases and demethylases
- Assay used to provide detailed insight into enzyme kinetics
- Demonstration of ability to profile small molecules inhibitors
- Mechanism of action of G9a inhibitors probed

Acknowledgments

We thank Dr. Feng Liu and Dr. Xin Chen for synthesizing the analogs of UNC0224, Amy Van Deusen for building compound plates and Irene Chau for providing the PRMT3 enzyme. We also acknowledge the efforts of Dr. Seth Cohen in facilitating this research. The project described was supported by Award Number RC1GM090732 from the National Institute Of General Medical Sciences, the Carolina Partnership, Caliper Life Sciences, the Ontario

Research Fund and the Structural Genomics Consortium, a registered charity (number 1097737) that receives funds from the Canadian Institutes for Health Research, the Canadian Foundation for Innovation, Genome Canada through the Ontario Genomics Institute, GlaxoSmithKline, Karolinska Institutet, the Knut and Alice Wallenberg Foundation, the Ontario Innovation Trust, the Ontario Ministry for Research and Innovation, Merck & Co., Inc., the Novartis Research Foundation, the Swedish Agency for Innovation Systems, the Swedish Foundation for Strategic Research and the Wellcome Trust.

References

Adams-Cioaba MA, Min J. Structure and function of histone methylation binding proteins. Biochem Cell Biol. 2009; 87:93–105. [PubMed: 19234526]

Boa S, Coert C, Patterton HG. Saccharomyces cerevisiae Set1p is a methyltransferase specific for lysine 4 of histone H3 and is required for efficient gene expression. Yeast. 2003; 20:827–835. [PubMed: 12845608]

Chang B, Chen Y, Zhao Y, Bruick RK. JMJD6 is a histone arginine demethylase. Science. 2007; 318:444–447. [PubMed: 17947579]

Chang Y, Zhang X, Horton JR, Upadhyay AK, Spannhoff A, Liu J, Snyder JP, Bedford MT, Cheng X. Structural basis for G9a-like protein lysine methyltransferase inhibition by BIX-01294. Nat Struct Mol Biol. 2009; 16:312–317. [PubMed: 19219047]

Chen X, Niroomand F, Liu Z, Zankl A, Katus HA, Jahn L, Tiefenbacher CP. Expression of nitric oxide related enzymes in coronary heart disease. Basic Res Cardiol. 2006; 101:346–353. [PubMed: 16705470]

Cole PA. Chemical probes for histone-modifying enzymes. Nat Chem Biol. 2008; 4:590–597. [PubMed: 18800048]

Collazo E, Couture JF, Bulfer S, Trievel RC. A coupled fluorescent assay for histone methyltransferases. Anal Biochem. 2005; 342:86–92. [PubMed: 15958184]

Copeland, RA. Enzymes: a practical introduction to structure, mechanism, and data analysis. 2. New York: J. Wiley; 2000.

Copeland RA, Solomon ME, Richon VM. Protein methyltransferases as a target class for drug discovery. Nat Rev Drug Discov. 2009; 8:724–732. [PubMed: 19721445]

Couture JF, Collazo E, Hauk G, Trievel RC. Structural basis for the methylation site specificity of SET7/9. Nat Struct Mol Biol. 2006; 13:140–146. [PubMed: 16415881]

Forneris F, Binda C, Vanoni MA, Battaglioli E, Mattevi A. Human histone demethylase LSD1 reads the histone code. J Biol Chem. 2005; 280:41360–41365. [PubMed: 16223729]

Friedman S. The effect of 5-azacytidine on E. coli DNA methylase. Biochem Biophys Res Commun. 1979; 89:1328–1333. [PubMed: 91371]

Frye SV. The art of the chemical probe. Nat Chem Biol. 2010; 6:159–161. [PubMed: 20154659]

Gelato KA, Fischle W. Role of histone modifications in defining chromatin structure and function. Biol Chem. 2008; 389:353–363. [PubMed: 18225984]

Huang J, Dorsey J, Chuikov S, Zhang X, Jenuwein T, Reinberg D, Berger SL. G9a and Glp methylate lysine 373 in the tumor suppressor p53. J Biol Chem. 2010; 285:9636–9641. [PubMed: 20118233]

Huang J, Sengupta R, Espejo AB, Lee MG, Dorsey JA, Richter M, Opravil S, Shiekhattar R, Bedford MT, Jenuwein T, et al. p53 is regulated by the lysine demethylase LSD1. Nature. 2007; 449:105–108. [PubMed: 17805299]

Karberg S. Switching on epigenetic therapy. Cell. 2009; 139:1029–1031. [PubMed: 20005793]

Keppler BR, Archer TK. Chromatin-modifying enzymes as therapeutic targets--Part 1. Expert Opin Ther Targets. 2008; 12:1301–1312. [PubMed: 18781828]

Kouzarides T. Chromatin modifications and their function. Cell. 2007; 128:693–705. [PubMed: 17320507]

Kubicek S, O'Sullivan RJ, August EM, Hickey ER, Zhang Q, Teodoro ML, Rea S, Mechtler K, Kowalski JA, Homon CA, et al. Reversal of H3K9me2 by a small-molecule inhibitor for the G9a histone methyltransferase. Mol Cell. 2007; 25:473–481. [PubMed: 17289593]

Li Y, Reddy MA, Miao F, Shanmugam N, Yee JK, Hawkins D, Ren B, Natarajan R. Role of the histone H3 lysine 4 methyltransferase, SET7/9, in the regulation of NF-kappaB-dependent

inflammatory genes. Relevance to diabetes and inflammation. J Biol Chem. 2008; 283:26771–26781. [PubMed: 18650421]

Liu F, Chen X, Allali-Hassani A, Quinn AM, Wasney GA, Dong A, Barsyte D, Kozieradzki I, Senisterra G, Chau I, et al. Discovery of a 2,4-diamino-7-aminoalkoxyquinazoline as a potent and selective inhibitor of histone lysine methyltransferase G9a. J Med Chem. 2009; 52:7950–7953. [PubMed: 19891491]

Marks PA. Discovery and development of SAHA as an anticancer agent. Oncogene. 2007; 26:1351–1356. [PubMed: 17322921]

Marmorstein R, Trievel RC. Histone modifying enzymes: structures, mechanisms, and specificities. Biochim Biophys Acta. 2009; 1789:58–68. [PubMed: 18722564]

Norvell A, McMahon SB. Cell biology. Rise of the rival. Science. 2010; 327:964–965. [PubMed: 20167774]

Quinn AM, Allali-Hassani A, Vedadi M, Simeonov A. A chemiluminescence-based method for identification of histone lysine methyltransferase inhibitors. Molecular BioSystems. 201010.1039/B921912A

Rathert P, Dhayalan A, Murakami M, Zhang X, Tamas R, Jurkowska R, Komatsu Y, Shinkai Y, Cheng X, Jeltsch A. Protein lysine methyltransferase G9a acts on non-histone targets. Nat Chem Biol. 2008; 4:344–346. [PubMed: 18438403]

Rea S, Eisenhaber F, O'Carroll D, Strahl BD, Sun ZW, Schmid M, Opravil S, Mechtler K, Ponting CP, Allis CD, et al. Regulation of chromatin structure by site-specific histone H3 methyltransferases. Nature. 2000; 406:593–599. [PubMed: 10949293]

Shi Y, Desponts C, Do JT, Hahm HS, Scholer HR, Ding S. Induction of pluripotent stem cells from mouse embryonic fibroblasts by Oct4 and Klf4 with small-molecule compounds. Cell Stem Cell. 2008a; 3:568–574. [PubMed: 18983970]

Shi Y, Do JT, Desponts C, Hahm HS, Scholer HR, Ding S. A combined chemical and genetic approach for the generation of induced pluripotent stem cells. Cell Stem Cell. 2008b; 2:525–528. [PubMed: 18522845]

Shi Y, Lan F, Matson C, Mulligan P, Whetstine JR, Cole PA, Casero RA. Histone demethylation mediated by the nuclear amine oxidase homolog LSD1. Cell. 2004; 119:941–953. [PubMed: 15620353]

Spannhoff A, Hauser AT, Heinke R, Sippl W, Jung M. The emerging therapeutic potential of histone methyltransferase and demethylase inhibitors. ChemMedChem. 2009a; 4:1568–1582. [PubMed: 19739196]

Spannhoff A, Sippl W, Jung M. Cancer treatment of the future: inhibitors of histone methyltransferases. Int J Biochem Cell Biol. 2009b; 41:4–11. [PubMed: 18773966]

Tahiliani M, Mei P, Fang R, Leonor T, Rutenberg M, Shimizu F, Li J, Rao A, Shi Y. The histone H3K4 demethylase SMCX links REST target genes to X-linked mental retardation. Nature. 2007; 447:601–605. [PubMed: 17468742]

Trewick SC, McLaughlin PJ, Allshire RC. Methylation: lost in hydroxylation? EMBO Rep. 2005; 6:315–320. [PubMed: 15809658]

Wigle TJ, Herold JM, Senisterra GA, Vedadi M, Kireev DB, Arrowsmith CH, Frye SV, Janzen WP. Screening for inhibitors of low-affinity epigenetic peptide-protein interactions: an AlphaScreen-based assay for antagonists of methyl-lysine binding proteins. J Biomol Screen. 2010; 15:62–71. [PubMed: 20008125]

Wu H, Min J, Lunin VV, Antoshenko T, Dombrovski L, Zeng H, Allali-Hassani A, Campagna-Slater V, Vedadi M, Arrowsmith CH, et al. Structural biology of human H3K9 methyltransferases. PLoS One. 2010; 5:e8570. [PubMed: 20084102]

Zhang JH, Chung TD, Oldenburg KR. A Simple Statistical Parameter for Use in Evaluation and Validation of High Throughput Screening Assays. J Biomol Screen. 1999; 4:67–73. [PubMed: 10838414]

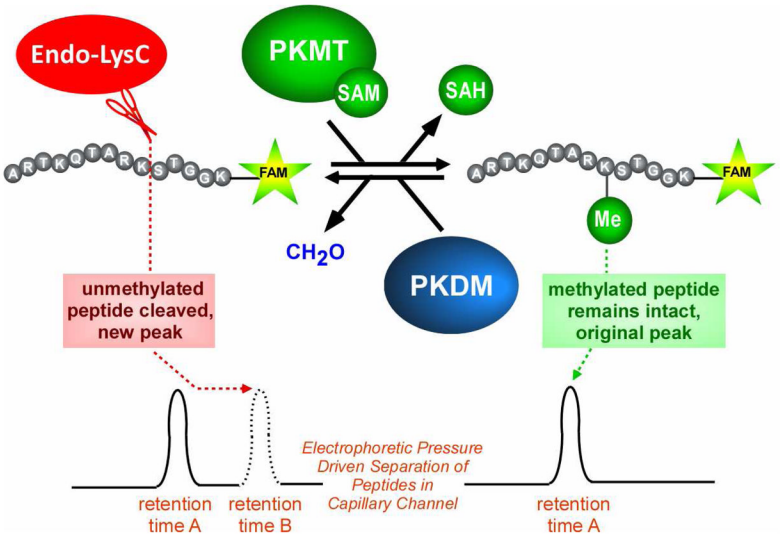

Figure 1. Methylation-Sensitive Endoproteinase-Linked Microfluidic Capillary Electrophoresis (MCE) Assay Concept

Protein lysine methyltransferases (PKMT) methylate substrate peptides, which prevents proteolysis of the peptide at the target lysine by Endoproteinase-LysC. Protein lysine demethylases (PKDM) demethylate peptide substrates and render it susceptible to proteolysis by Endoproteinase-LysC. The cleaved vs. uncleaved peptides are separable on a Caliper Life Sciences EZ Reader II, which “sips” nanoliter-sized samples from reactions in microplate wells into a capillary channel on a quartz chip. A pressure driven flow and electric current are used to resolve the peptides based on their charge-to-mass ratio. The incorporation of a fluorescein-based tracer enables the detection of the peptides at the end of the capillary channel. This assay format is compatible with 384-well microplates, can be performed in volumes as low as 10–15 μL and is a widely-used technology in drug discovery.

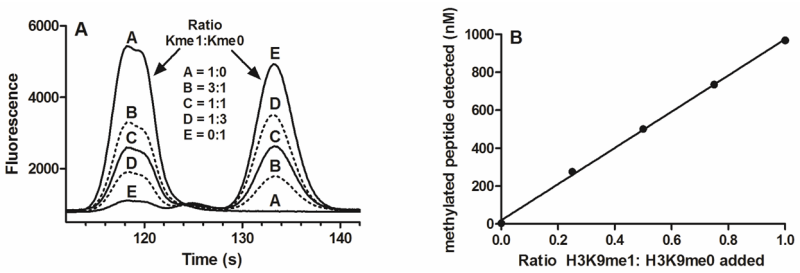

Figure 2. Separation of Histone H3 Peptides Representative of Unmethylated and Monomethylated Lysine 9 on the Caliper EZ Reader II

Ratios of H3K9me0 (peptide **1**) and H3K9me1 (peptide **5**) adding up to 1 μM total peptide were mixed and Endo-LysC was added. After 1h, the products were separated on the Caliper EZ Reader II. (A) The direct readout from the EZ Reader II showing the separation of products “sipped” from the 384-well plate containing titrations of the H3K9me1 to H3K9me0 peptide. (B) A correlation plot of the experimentally detected amount of methylated peptide detected vs. the calculated ratio of methylated to unmethylated peptides added.

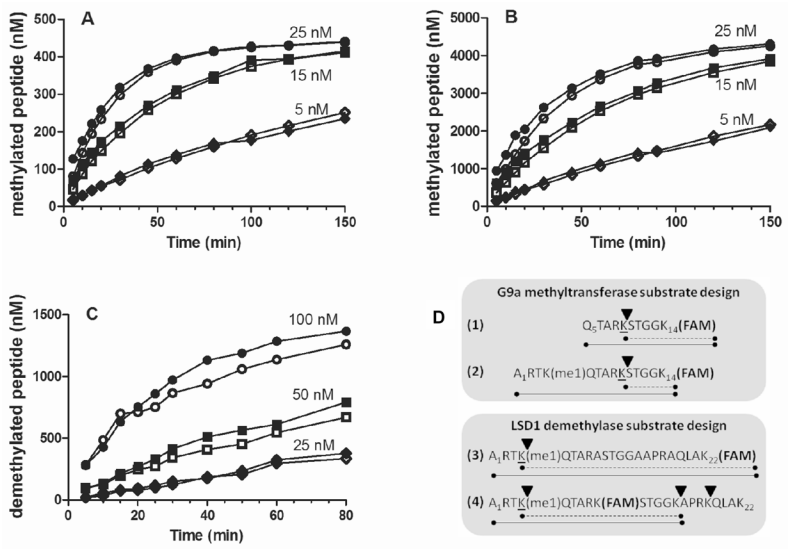

Figure 3. Substrate Design and Activity Measured for G9a Methyltransferase and LSD1 Demethylase Enzymes Using the MCE Assay Platform

Activity of G9a and LSD1 with heatkill (open symbols) or direct addition to Endo-LysC (closed symbols) to terminate the reaction. G9a and LSD1 were present at three different concentrations as indicated on the plots. (A) G9a reaction with 500 nM of peptide **2** present. (B) G9a reaction with 5000 nM of peptide **2** present. (C) LSD1 reaction with 2000 nM peptide **4**. (D) Pairs of initial and optimized histone H3 peptide substrate designs for G9a and LSD1 enzymes. Endo-LysC susceptible sites are indicated by triangles and lysine residues targeted by G9a or LSD1 are underlined. The 5/6-FAM group in each peptide is attached to the lysine ε-amino group, indicated by the K**(FAM)** designation. The detected substrate (solid line) and product (dashed line) species resulting from Endo-LysC digestion are indicated beneath the peptide sequences.

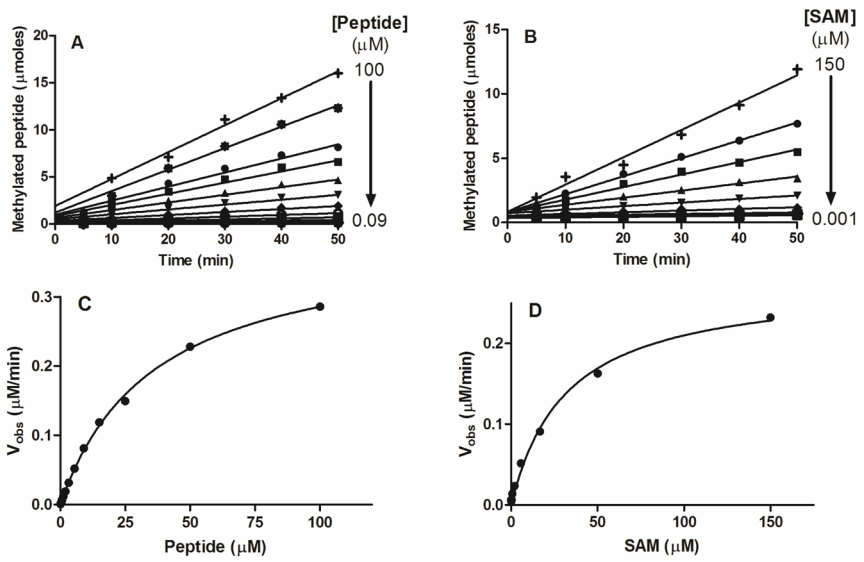

Figure 4. Determination of K_m and V_{max} With Respect to Peptide 2 or SAM in the G9a MCE Assay

Peptide **2** or SAM were titrated by the indicated amounts and timepoints were taken at fixed intervals so that reaction velocity could be determined and Michaelis-Menten kinetics were plotted. (A) & (C), the peptide titration indicates a $K_m^{peptide}$ of 36.2 μM and k_{cat} of 15.5 min^{-1}. (B) & (D), the SAM titration indicates a K_m^{SAM} of 31.7 μM and k_{cat} of 11.1 min^{-1}. The standard error of the mean in 3 separate reactions is indicated by error bars in (A) & (B).

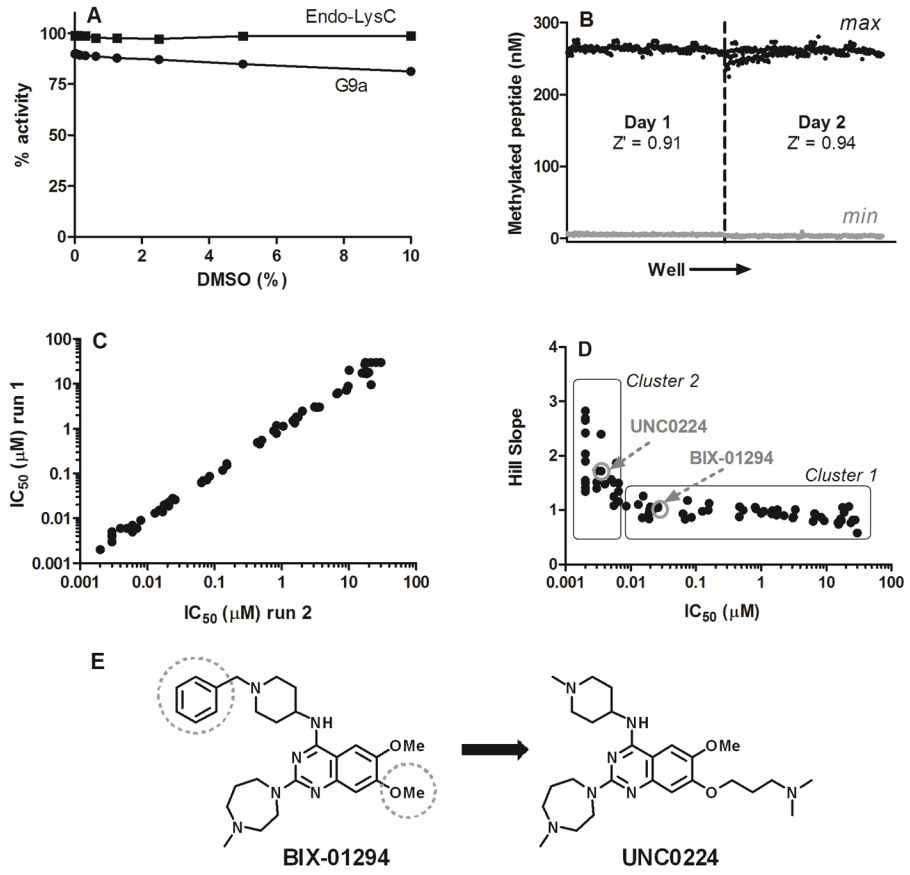

Figure 5. Configuring the G9a MCE Assay for Small Molecule Screening

(A) DMSO sensitivity curves for G9a and Endo-LysC. (B) Statistical evaluation of the maximum and minimum signal control reactions of the assay over the course of two days results in an average Z′ factor of 0.92 and CV's of less than 2%. (C) Graphical representation of the IC_{50} values measured for 83 small molecules over the course of two independent runs of the assay indicates excellent correlation between dose response assays. (D) A plot of Hill Slope vs. the IC_{50} measured indicates two major clusters of compounds: (1) Compounds with Hill Slope of roughly 1 and potency > 5 nM are rank-ordered by the assay, (2) while compounds with Hill Slope > 1 and IC_{50} < 5 nM have reached the potency detection limit of the assay. UNC0224 and BIX-01294 are indicated on the plot. The observation that IC_{50} values of as little as 2 nM can be measured is likely a reflection of the fraction of active G9a among the 10 nM enzyme added. (E) Structure guided design of UNC0224 from the BIX-01294 quinazoline template.

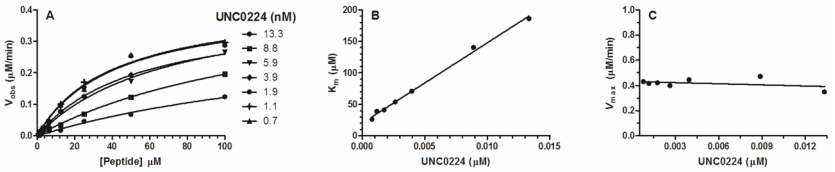

Figure 6. Measuring a K_i for the Known Peptide-Competitive G9a Methyltransferase Inhibitor UNC0224

(A) The velocity of the reaction was determined by analyzing 6 timepoints spanning 100 minutes, and analyzed by linear regression to determine the V_{obs} values. (B) The measured K_m^{obs} and V_{max} values plotted as a function of UNC0224 concentration.

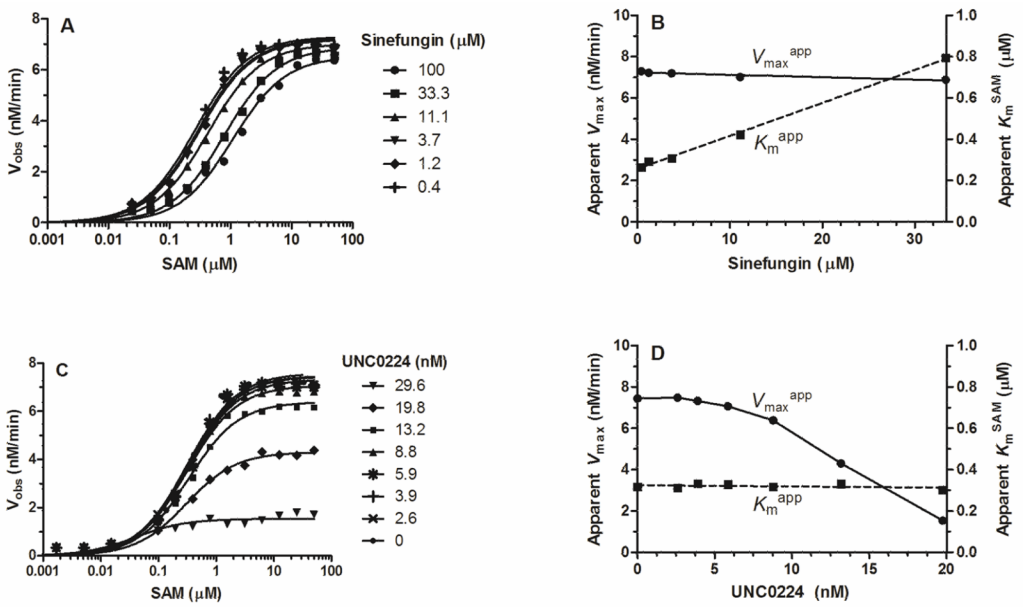

Figure 7. A Rapid End-Point Method for the Assessment of Competition With Respect to SAM in G9a Methyltransferase MCE Assay

To conserve reagent, we determined the influence of inhibitors on SAM-dependent kinetic parameters using less-than-saturating peptide, finding a quick and effective way to fingerprint hits for an inhibitory mechanism of action. (A) & (B) The SAM analog, Sinefungin exhibited the increased K_m^{app} and constant V_{max}^{app} that are hallmarks of a SAM-competitive inhibitor and yielded a K_i^{app} of 18 μM. (C) & (D) The peptide-competitive inhibitor UNC0224 does not alter the K_m^{app}, but results in asymptotically decreasing V_{max}^{app}, traits which are indicative of an inhibitor that is non-competitive with SAM.